

# Search for Dark Matter in the Upgraded High Luminosity LHC at CERN

Sensitivity of ATLAS phase II upgrade to dark matter production

Sven-Patrik Hallsjö

June 3, 2014

1 / 34

## Introduction

### Who am I?

- 5th year Y-programme student.
- Defending a 30hp Masters thesis in applied physics.

### Project

- The theses work was performed at Stockholm University. It started January 7th and ended May 16th (19 weeks).
- The work was done with the ATLAS group at the University looking at the sensitivity for dark matter production after the phase II upgrade.

2 / 34

## Goals

- Compare observables before and after smearing. What observables are the least/most affected?
- Implement selection criteria that select the signal collisions efficiently while significantly reduce the background.
- Calculate the figure of merit  $p$  for the given selection criteria before and after smearing.
- Investigate other selection criteria and observables, to mitigate the effect of high luminosity. Use  $p$  to rank different criteria after smearing.
- Conclude on the effect of the high luminosity on the sensitivity for dark matter and possible ways to mitigate its effects using alternative observables and selection criteria.

3 / 34

## Dark matter

### What is dark matter?

- Looking outside of our solar system it is seen that the rotational speed of galaxies does not increase, as expected, with distance to the rotational center, it is instead constant.
- Dark matter is the name given to, among other things, one solution to the discrepancies of galactic rotations.

### Properties

All that is known so far is given in the name Dark matter.

- Dark, no electromagnetic interaction.
- Matter, have gravitational interactions.

It is known that it can not be made up by anything in the standard model of particle physics, thus a new physical description is needed to explain dark matter.

4 / 34

## Dark matter

There are several strategies to search for dark matter, the main one in this thesis is:

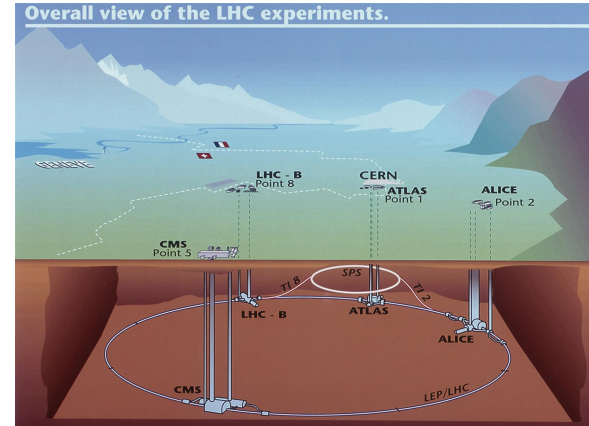
- Ordinary matter interacting with ordinary matter can produce dark matter, known as production. This is the process which occurs in particle accelerators and is the method explored in this thesis.

5 / 34

## LHC

The large hadron collider (LHC) is a particle accelerator located at CERN near Geneva in Switzerland.

Overall view of the LHC experiments.

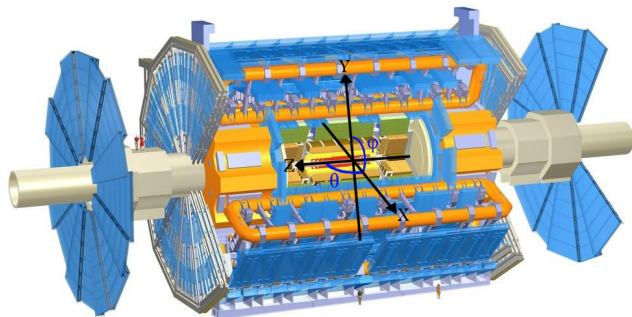


6 / 34

## ATLAS

### ATLAS

The ATLAS detector is a general purpose detector that uses a toroid magnet. Its goal is to observe several different production and decay channels



7 / 34

## Dark matter in particle collisions

- There are two main classes of events, signal and background.
- The signal corresponds to events that would arise from one of the DM processes.
- It will not be possible for the ATLAS detector to directly detect dark matter signals, it will only be detected as missing energy through a mono-jet analysis.
- ATLAS has looked at proton-proton collisions, with 8 TeV center of mass energy,  $\sqrt{s}$ , which contain high energetic jets without finding any excess of mono-jet events.
- What is a mono-jet analysis?

8 / 34

## Mono-jet event

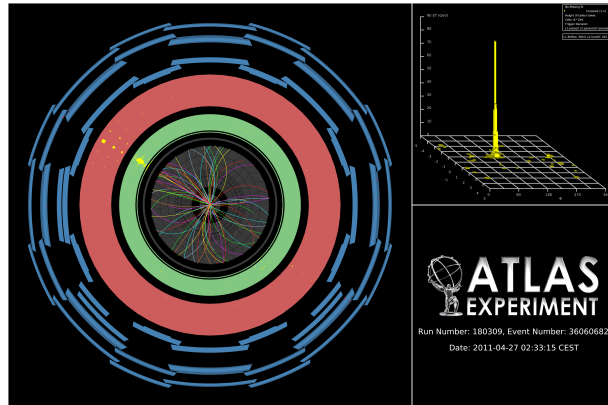


Image in the transverse plane of a mono-jet event recorded by the ATLAS experiment. The figure in the top right is a diagram in the  $(\eta, \varphi)$ -plane showing where in the calorimeter (red in the main figure) the energy is deposited and how much.

9 / 34

## Mono-jet analysis

- Conservation of momentum in the transverse plane of the experiment indicates that the sum of all momenta should be zero as before the collision.
- Since there is no balancing jet there must be transverse energy that is not detected, denoted  $E_T^{Miss}$ , indicating that the energy to balance this can not be detected. This could for instance be the characteristic signature of dark matter.

### Definition of $E_T^{Miss}$

$E_T^{Miss}$  is the modulus of the  $\vec{E}_T^{Miss}$  vector which is defined as:

$$\vec{E}_T^{Miss} = -\sum \vec{p}_T^{Jet} - \sum \vec{p}_T^{Electron} - \sum \vec{p}_T^{Muon} - \sum \vec{p}_T^{Tau} - \sum \vec{p}_T^{Photon}$$

where  $p_T$  denotes the transverse momenta and the superscripts denote the detectable particles in the detector.

10 / 34

## Phase II upgrade

At the moment, the whole LHC is undergoing a step by step upgrade program which will be finalized around 2022-2023, denoted the high luminosity upgrade, or HL-upgrade. The upgrade consists of different stages, meaning that the upgrade will halt for periods so that experiments can take place.

The upgrade in focus in this thesis is known as phase II and will be implemented between 2021 and 2022-2023. It will increase the center of mass energy for the colliding particles to 14 TeV and the rate at which these are collided. The amount of data collected will also increase to  $1000 fb^{-1}$ .

The increase in collision events, instantaneous luminosity [ $fb^{-1}s^{-1}$ , 1 barn( $b$ )=  $10^{24} cm^2$ ], will unfortunately lead to events occurring simultaneously known as pile-up.

11 / 34

## Simulation of particle collisions

For the phase II upgrade there does not exist a full simulation of the detector. This thesis instead uses data from Monte Carlo simulations for the particle collisions and then uses so called smearing functions to emulate the detector responses.

- The MC simulation, based on probability calculation from quantum mechanics, is denoted as truth data.
- Data after the smearing is denoted reconstructed data or reco data and would be compared to measured data if there were any.

12 / 34

## Validation of smearing functions

- The smearing functions are the official functions developed from previous studies by the ATLAS collaboration for the study of the ATLAS phase II upgrade.
- The key result of those studies was that the direction of the momenta is unaffected and that only jets and  $E_T^{Miss}$  are affected by pile-up.
- Since this was confirmed in previous studies it was not incorporated into the smearing functions.
- The first step of the project was to validate that these functions were implemented and functioned correctly.

13 / 34

## Smearing functions

- In a simulation of a proton-proton collision all quantities such as energy, momentum and direction of all produced particles are perfectly known.
- In a real experiment it is only possible to get measured values from the detector.
- The detector energy and momentum resolutions given in the smearing functions relate the measured values to the truth values on a statistical basis as given below.

$$E' = E + \Delta E = E + \sigma$$

where  $E$  is the energy at a truth level and  $E'$  is the smeared energy and  $\Delta E$  or  $\sigma$  is a random number obtained by sampling a Gaussian distribution with mean value 0 and a standard deviation equal to the resolution for that particle, and will be denoted  $\sigma$ .

14 / 34

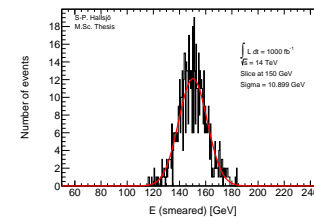
## Validation

Since part of this thesis work is to take the official atlas smearing functions and apply the smearing to each particle, it is important to check that the energy and momenta resolutions of the smeared objects are consistent with the expected measured values.

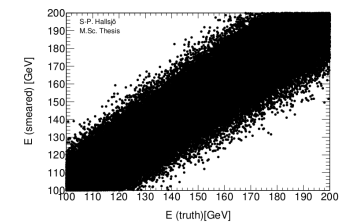
15 / 34

## Validation

In 1a the Gaussian fit (red) and the data (black) are given for tau detected through 3 prong. In 1b smeared energy is plotted against truth energy.



(a) Tau energy after smearing.



(b) Tau smeared vs truth.

Figure : Tau energy after smearing and smeared vs truth.

16 / 34

## Conclusion

The smearing functions work as intended within 5.8 sigma, however when using a test box and averaging the sigmas one ends up with half of this for the extreme cases, muons and  $E_T^{Miss}$ . This indicates that the statistical fluctuation of these values and of the error calculations are considerable. Even with this statistical fluctuation the smearing functions work as intended.

17 / 34

## Sensitivity to dark matter signals

### Main part of the project

With the validation completed focus turned to investigating the signal models. The following tasks were set and performed.

- Compare background simulation to previous measured data.
- Evaluate the limit of the mass suppression scale of the D5 operator model.
- Evaluate the limit of the mediator mass of the light vector mediator model.

18 / 34

## Comparing events

### Signal regions

- To compare data, signal regions are used.
- These are restrictions on certain parameters to minimize unwanted data. These are not known a priori and must be designed depending on what is interesting.

19 / 34

## Signal regions

The pre-selection criteria used in Ref. ATLAS-CONF-2012-147 are the following:

- Jet veto, require no more than 2 jets with  $p_T > 30\text{GeV}$  and  $|\eta| < 4.5$ . This is done to reduce the number of multi-jet events.
- Lepton veto, no electron or muon. These vetos are there to remove uninteresting  $W \rightarrow e\nu$  and  $W \rightarrow \mu\nu$  background events.
- Leading jet with  $|\eta| < 2.0$  and  $\Delta\varphi(\text{jet}, E_T^{Miss}) > 0.5$  (second-leading jet). This is done to further reduce the number of multi-jet events.

The following signal regions were used:

signal region	SR3p	SR4p
minimum leading jet $p_T$ (GeV)	350	500
minimum $E_T^{Miss}$ (GeV)	350	500

Table : The signal regions from Ref. ATLAS-CONF-2012-147.

20 / 34

## Signal regions

The proposed pre-selection criteria differ in the veto:

- Electron veto which is defined:  $\Delta R(jet^{lead}, electron^{lead}) \geq 0.4$  and  $electron^{lead} p_T > 20 \text{ GeV}$  removed.
- Muon veto which is defined:  $\Delta R(jet^{lead}, muon^{lead}) \geq 0.4$  and  $muon^{lead} p_T > 20 \text{ GeV}$  removed.

These formulation of vetos are used to remove uninteresting  $W \rightarrow e\nu$  and  $W \rightarrow \mu\nu$  background events without removing too much of the signal. The  $\Delta R$  involvement is to make sure that the veto is only on simulated true particles and not simulated false detections.

Here the superscript lead denotes the entity with highest transverse momentum  $p_T$ . Thus  $electron^{lead}$  would be the simulated electron in an event with the highest  $p_T$ .

21 / 34

## Signal regions

To try and minimize the amount of background compared to the amount of signal, the following signal regions are used:

Symmetric signal region	SR1	SR1p	SR2	SR3	SR4
minimum leading jet $p_T$ (GeV)	350	500	600	800	1000
minimum $E_T^{Miss}$ (GeV)	350	500	600	800	1000
Asymmetric signal region	SRa	SRb	SRc	SRd	
minimum leading jet $p_T$ (GeV)	350	350	350	350	
minimum $E_T^{Miss}$ (GeV)	350	600	800	1000	

Table : The new signal regions.

22 / 34

## Comparing with a previous paper

### Comparison

To make sure that the utilized background is correct, it is compared to the background from the article:  
ATLAS-CONF-2012-147, Search for New Phenomena in Monojet plus Missing Transverse Momentum Final States using 10fb-1 of pp Collisions at  $\sqrt{s} = 8 \text{ TeV}$  with the ATLAS detector at the LHC.

For the comparison to be done, samples of data comparable to measured data needed to be used.

23 / 34

## Comparing with a previous paper

	SR3p		SR4p	
Process	Work	Paper	Work	Paper
$Z \rightarrow \nu\nu$	140298	152000	25250	27000
$W \rightarrow \tau\nu$	40701	37000	5862	3900
$W \rightarrow e\nu$	11229	11200	1507	1600
$W \rightarrow \mu\nu$	13727	15800	1872	4200
Total background	205955	218000	34491	36700

Table : Comparison of the simulated events with expected events from ATLAS-CONF-2012-147 with  $L = 1000\text{fb}^{-1}$ , cross-sections corresponding to  $\sqrt{s} = 8\text{TeV}$  and using the same electron and muon veto.

	SR1		SR1p	
Process	Work	Paper	Work	Paper
$Z \rightarrow \nu\nu$	150753	152000	27569	27000
$W \rightarrow \tau\nu$	49320	37000	7318	3900
$W \rightarrow e\nu$	18329	11200	2534	1600
$W \rightarrow \mu\nu$	22290	15800	3218	4200
Total background	240690	218000	40639	36700

Table : Comparison of the simulated events with expected events from ATLAS-CONF-2012-147 with  $L = 1000\text{fb}^{-1}$ , cross-sections corresponding to  $\sqrt{s} = 8\text{TeV}$  and using a modified electron and muon veto.

24 / 34

## Conclusion from comparison

### Background

- The background is similar.
- $\tau$  is higher since there is no way for  $\tau$  to be reconstructed as jets in the code, with the cut above this will have a large impact.  $\phi(secondleadingjet, E_T^{miss}) > 0.5$
- The veto needed to change for the signal to survive.
- In the proposed there is no veto on false detections.

Since the background is validated, the signals can be evaluated.

25 / 34

## Compare signal to background

### Sensitivity

- Measured as the probability of having the background fluctuate to S+B.
- If  $p < 0.05$  then we have sensitivity.

To compute sensitivity at 14 TeV need to make assumptions about uncertainties in the background events.

Use  $10 \text{ fb}^{-1}$  mono-jet paper as baseline.

- In total the error is either, 0.08 or 0.02.

26 / 34

## D5 operator model

### D5

The operator is based on the assumption that the mediator between dark matter and ordinary matter acts like a heavy z-boson.

### Mass suppression scale limit

The cross-section, related to the probability of the process is scaled for D5 using  $M^*$  as,  $\sigma(M^*) = (\frac{\sigma_{ref}}{M^*})^4$  where  $\sigma_{ref}$  is the theoretically calculated value.

The goal is to find the value of  $M^*$  for which  $p=0.05$  when compared to the background.

### Available models

Two different models, one with an assumed dark matter mass of 50 GeV and the other at 400 GeV are evaluated.

27 / 34

## D5 operator model

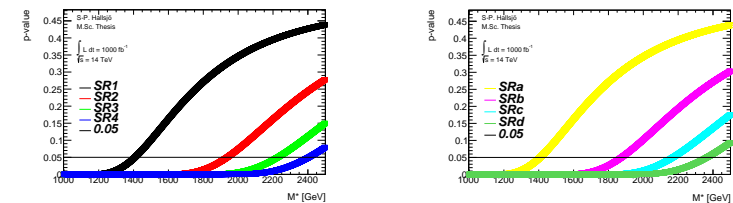


Figure : p-value as a function of the mass suppression scale  $M^*$  at truth level for error model 0.02.

28 / 34

## Conclusion

Increasing the centre of mass energy will increase the limits by a factor of 2-3.

Dark matter mass	From simulation	From paper
50 GeV	1960 GeV	800 GeV
400 GeV	1871 GeV	700 GeV

Table :  $M^*$  values in SR2 from both simulation at 14 TeV,  $1000\text{fb}^{-1}$  and from 8 TeV and  $10\text{fb}^{-1}$ .

29 / 34

## Light vector mediator model

### Models

In this thesis these signals have two different width scenarios,  $M/3$  and  $M/8\pi$  where  $M$  denotes the mediator mass. The width scenarios contain eight different mediator mass scenarios with masses between 100 and 15000 GeV. In addition to this there are, as with the D5 operator, two different dark matter masses, one at 50 GeV and one at 400 GeV.

30 / 34

## Light vector mediator model

width	$m_\chi = 50 \text{ GeV}$	$m_\chi = 400 \text{ GeV}$
$M/3$	1000 GeV	1000 GeV
$M/8\pi$	3000 GeV	3000 GeV

Table : Limits on the highest mediator mass model which can be excluded for different widths, different dark matter masses for truth and reconstructed data and both error models in SR2, 3, 4, c, d.

width	$m_\chi = 50 \text{ GeV}$	$m_\chi = 400 \text{ GeV}$
$M/3$	1000 GeV	1000 GeV
$M/8\pi$	1000 GeV	1000 GeV

Table : Limits on the highest mediator mass model which can be excluded for different widths, different dark matter masses for truth and reconstructed data and both error models in SRb.

31 / 34

## Final conclusion

### Limit on $M^*$

The limits can be found in subsection 3.3.3 and are 2-3 times better than previous results at 8 TeV and  $10\text{fb}^{-1}$ .

### Limit on mediator mass models

The limits are found in the previous slide and are the first result done with these models and thus can not be compared. Effect of the high luminosity

### Pile-up

The effect of increased pile-up is at most  $< 5\%$  compared to truth level on the mass suppression scale and does not affect the vector mediator models limits.

32 / 34



## Final remarks

The most interesting continuation of this work would be to compare the results given here to measurements done after the phase II upgrade, and hopefully see characteristic signatures from dark matter.

33 / 34

## Thank you

Thank you for your attention.

34 / 34

## Backup

34 / 34

## Summary of validation

Process	$\eta$ value	Pile-up value	$\sigma$ [GeV]	Expected $\sigma$ [GeV]
Electron	Low $\eta$	60	$1.25 \pm 0.05$	1.18
	High $\eta$	60	$1.82 \pm 0.14$	1.74
Photon	Low $\eta$	60	$1.19 \pm 0.04$	1.18
	High $\eta$	60	$1.80 \pm 0.04$	1.74
Muon	Low $\eta$	60	$1.19 \pm 0.05$	1.50
	High $\eta$	60	$1.71 \pm 0.09$	2.18
Tau	All $\eta$	60	$10.9 \pm 0.3$	10.3
Jet	Low $\eta$	60	$11.4 \pm 0.4$	11.6
	Low $\eta$	140	$15.4 \pm 0.5$	15.8
	Mid low $\eta$	60	$11.5 \pm 0.5$	11.9
	Mid low $\eta$	140	$15.1 \pm 0.7$	15.9
	Mid high $\eta$	60	$11.3 \pm 0.3$	10.9
	High $\eta$	60	$16.6 \pm 1.5$	13.5
$E_T^{Miss}$	All $\eta$	60	$43 \pm 2$	48
	All $\eta$	140	$105 \pm 12$	87

Table : Calculated  $\sigma$  values compared to  $\sigma$  given from the resolution. Values are given at different pile-up values for comparison.

34 / 34

## D5 operator model

Signal region	Truth [GeV]	Reconstructed [GeV]
SR1, symmetric 350 GeV	1407	1402
SR2, symmetric 600 GeV	1936	1934
SR3, symmetric 800 GeV	2227	2226
SR4, symmetric 1000 GeV	2404	2406
SRa, asymmetric 350 GeV	1425	1421
SRb, asymmetric 600 GeV	1874	1803
SRc, asymmetric 800 GeV	2169	2125
SRd, asymmetric 1000 GeV	2365	2340

**Table :** Limits on mass suppression scales in GeV given for  $m_\chi = 50$  GeV and the 0.02 error model.

## D5 operator model

Signal region	Truth [GeV]	Reconstructed [GeV]
SR1, symmetric 350 GeV	1333	1329
SR2, symmetric 600 GeV	18481	1847
SR3, symmetric 800 GeV	2162	2163
SR4, symmetric 1000 GeV	2332	2303
SRa, asymmetric 350 GeV	1350	1346
SRb, asymmetric 600 GeV	1789	1721
SRc, asymmetric 800 GeV	2106	2059
SRd, asymmetric 1000 GeV	2288	2258

**Table :** Limits on mass suppression scales in GeV given for  $m_\chi = 400$  GeV and the 0.02 error model.